Magnetic, chemical and radionuclide studies of river sediments and their variation with different physiographic regions of Bharathapuzha River, southwestern India

MARCOS A.E. CHAPARRO[1], NANJUNDAN KRISHNAMOORTHY[2,3], MAURO A.E. CHAPARRO[1,4], KARINA L. LECOMTE[5], SUNDARAM MULLAINATHAN[6], ROHIT MEHRA[7] AND ANA M. SINITO[1]

1 Centro de Investigaciones en Física e Ingeniería del Centro de la Provincia de Buenos Aires (CIFICEN, CONICET-UNCPBA), Pinto 399, 7000 Tandil, Argentina (chapator@exa.unicen.edu.ar)

2 Research and Development Centre, Bharathiar University, 641 046 Coimbatore, Tamilnadu, India

3 Department of Physics, CSI College of Engineering, 643 215 Ketti, Tamilnadu, India

4 Departamento de Matemáticas, Facultad de Ciencias Exactas y Naturales UNMDP, Mar del Plata, Argentina

5 Centro de Investigaciones en Ciencias de la Tierra (CICTERRA), CONICET and Universidad Nacional de Córdoba. Av. Vélez Sarsfield 1611, X5016GCA Córdoba, Argentina

6 Department of Physics, AVC College of Engineering, 608 002 Mayiladuthurai, Tamilnadu, India

7 Department of Physics, Dr B R Ambedkar National Institute of Technology, 144 011 Jalandhar, India

Received: July 8, 2014; Revised: September 29, 2014; Accepted: January 13, 2015

ABSTRACT

Bharathapuzha River is the second longest river in southwest India, where three physiographic regions show a distinctive spatial variation and their bed sediments can be considered environmental hosts for end-products generated by human activities and natural radionuclide components. Thus, the study of this river sediments in SW India is important not only because they are recorders of adverse human impacts (e.g., intense agricultural activities and urban pollution), but also because of their potential health hazards due to their common use as construction materials. Magnetic (e.g., magnetic susceptibility, anhysteretic remanent magnetisation and isothermal remanent magnetisation), radionuclide (^{226}Ra, ^{232}Th and ^{40}K) and chemical (trace and major elements) measurements were carried out in bed sediment samples along 33 sites from the uppermost catchment downstream. Magnetic measurements show the dominance of ferrimagnetic minerals; their concentration ranges widely along the river and between regions, showing up to 7-fold higher values for concentration-dependent magnetic parameters, e.g., mean values of saturation of isothermal remanent magnetisation acquisition are 67.9 and 9.4×10^{-3} $Am^2 kg^{-1}$ for highland and lowland regions,

respectively. Multivariate statistical analyses show the existence of relationships between magnetic, radioactivity and chemical variables. In particular, magnetic concentration-dependent parameters are significantly correlated with radioactivity variables ^{40}K and ^{226}Ra (with concentrations about 20% higher than the worldwide mean values), as well as with some elements: Fe, Ca and P. Such analyses also show differences between physiographic regions where samples from the highland (and lowland) region are well grouped showing higher (lower) magnetic concentrations and lower (higher) coercivity minerals. The spatial variation of magnetic parameters along the river can be related to the influence of both natural sources and human activities, i.e. urbanisation and intense agricultural activities. In this sense, environmental magnetism data provide very useful tools to investigate adverse human activities occurring in the riverine environment.

Keywords: magnetic parameters, major and trace elements, multivariate statistical

1. INTRODUCTION

Rivers play a significant role in modifying the landscape. They carry dissolved and particulate elements and sediments from their sources and deposit them sequentially based on their physicochemical characteristics. In India, mostly in South India, river sediments are used primarily for the construction of buildings. River bed sediments can be considered an environmental host for many chemical, biological, radionuclide and aquatic waste products discharged by humans because air and water pollution by different components are deposited in the sediments. Land environments suffer a major impact because hazardous components are transferred to the Earth's surface, made available, and taken-up by organisms or incorporated into sediments. Thus, the knowledge and detailed understanding of the various types of these components are essential to humans in monitoring the environmental changes by natural background radiation (radioactive elements) and anthropogenic activities emitting particulate matter, heavy metals, and persistent organic pollutants (*El-Bahi, 2004*; *El-Gamal et al., 2007*; *Evans and Heller, 2003*). Trace elements (as toxic metals) are introduced into agricultural soils by cultivation practices such as fertilisation, irrigation, pesticide application and organic waste disposal (*Chen et al., 2007*, *Chauhan et al., 2013*). Moreover, as it is widely known, human actions also play a mixed role: they increase erosion by employing inadequate soil use practices and, in contrast, they retain sediments behind dams. For example, dam constructions in a river interrupt the water flow and sediment transport; hence, the river adjusts its channel morphology. Such morphologic changes include: sediment deposition and channel aggradation upstream of the dam; channel degradation downstream of the dam; and coarsening of surface sediment particles and reduced sediment mobility downstream of the dam. *Milliman and Farnsworth (2011)* have thoroughly investigated this aspect. This additional anthropogenic impact adds complexity to the current scenario.

Magnetic techniques in environmental magnetism have been successfully developed and improved, becoming a very useful tool in order to investigate and understand the processes occurring in different environments (*Petrovský and Ellwood, 1999*). A large number of exhaustive studies of magnetic proxies for pollution have been conducted in different environments, including soils, sediments, and vegetation, since the 1980s (e.g., *Hunt et al., 1984*; *Beckwith et al., 1986*; *Thompson and Oldfield, 1986*). Magnetic

parameters have been widely used in environmental magnetism and some of them have been proven to be good proxies for environmental changes and contamination. Thus, magnetic proxies allow rivers to be assessed for reduced or wide extensions using the bed sediments (e.g., *Scholger, 1998*; *Magiera et al., 2002*; *Jordanova et al., 2004*; *Desenfant et al., 2004*; *Chaparro et al., 2004, 2008, 2013*; *Knab et al., 2006*; *Yang et al., 2007*; *Franke et al., 2009*; *Zhang et al., 2011*; *Sandeep et al., 2011*).

The study of natural radioactivity in sediments provides information about the nature of radionuclides in aquatic environments and the health hazards due to such radionuclides. Some investigations have shown the dependence of radionuclide concentrations on grain size, magnetic minerals, composition or organic content (*Bulman et al., 1984*, *De Meijer et al., 1985, 1990*; *Elejalde et al., 1996*; *Watson and Ellwood, 2001*). Radionuclides can be included in minerals, which are transported through erosive processes and can reach the river and coast, becoming part of the sediments (*Ligero et al., 2001*). In case both minerals and radionuclides can be assumed to be dispersedly found and similar affected by the process, correlation between the major minerals and the radionuclides may be expected. *McCubbin et al. (2004)* assessed the association of α-emitting radionuclides with iron minerals in beach sands that were subjected to successive extractions to separate magnetic iron oxide minerals. They found that radionuclide concentrations in the magnetic extracts were enhanced (4–6-fold) relative to the residue. However, they found no evidence of preferential association of radionuclides with ferrimagnetic minerals compared with antiferromagnetic minerals. *Montes et al. (2012)* found in coastal soils that Mössbauer-relative areas (Fe species: magnetite and haematite) are negatively correlated with ^{226}Ra and ^{40}K activities. Recently, in river sediments from southeastern India, *Ramasamy et al. (2014)* reported in Vaigai River significant positive correlations between mass-specific magnetic susceptibility χ and the concentration of ^{232}Th and ^{238}U. In addition, in Ponnaiyar River, *Suresh et al. (2011)* also reported that χ and the content of clay minerals are positively correlated with the concentration of ^{232}Th and ^{40}K, but negatively correlated with the concentration of ^{238}U. They found that the activity concentration depends upon the content of clay minerals (kaolinite). The presence of large thorium concentration is due to weathering of rocks from the Nilgiri Hills, Tamilnadu.

Previous studies in Bharathapuzha River showed mean values of χ higher than in others rivers of southern India, such as Palaru, Cauvery, Vellar and Ponnaiyar rivers (*Chaparro et al., 2008, 2011, 2013*). Furthermore, *Krishnamoorthy et al. (2014)* found statistically significant correlations between χ and the activity concentration of natural radionuclides (^{40}K and ^{226}Ra). They found that higher concentrations of both radionuclides may be associated with the extensive exploitation of phosphate and potassium fertilisers in the surrounding agricultural area. A constituent of these fertilisers is phosphorus, which is obtained from the treatment of phosphate rocks. By processing phosphate rock to fertiliser, the radioactivity of the ore is transferred to the product and to waste products (*Scholten and Timmermans, 1996*). One of the sources of radioactivity, other than those of natural origin, is mainly due to extensive use of fertilisers; among a number of studies, *Chauhan et al. (2013)* reported that different fertilisers (e.g., potash fertiliser, nitrogen phosphorous potassium, zinc sulphate, organic fertiliser, etc.) contain an enhanced concentration of natural radionuclides, the presence of major elements, as well as fluorapatite, hydroxylapatite, chlorapatite and iron oxides.

In this study, detailed magnetic properties of bed sediments from Bharathapuzha River are reported. It is of interest for this contribution to assess the distribution of magnetic minerals and other components along the river, which allowed the classification of sites and their adverse influence on the environment. In addition, the study of relationships between magnetic minerals, radionuclides, major and trace elements is also of interest in order to investigate the use of magnetic parameters as environmental proxies.

2. GEOLOGICAL SETTINGS

The Bharathapuzha River has a length of 209 km and originates in the Annamalai Hills located in the Western Ghats region in Tamil Nadu. The hydrological basin lies approximately between 10°26′N and 11°13′N and 75°53′E to 77°13′E. For the first 40 km, Bharathapuzha River flows northwards until Pollachi in the Coimbatore District, Tamilnadu State. The Kannadippuzha and Kalpathippuza (tributaries of Bharathapuzha) meet at Parli, and then it flows westwards to end at Ponnani in the Arabian Sea, draining through Palakkad and Malappuram Districts in Kerala State (Fig. 1). There are nine main

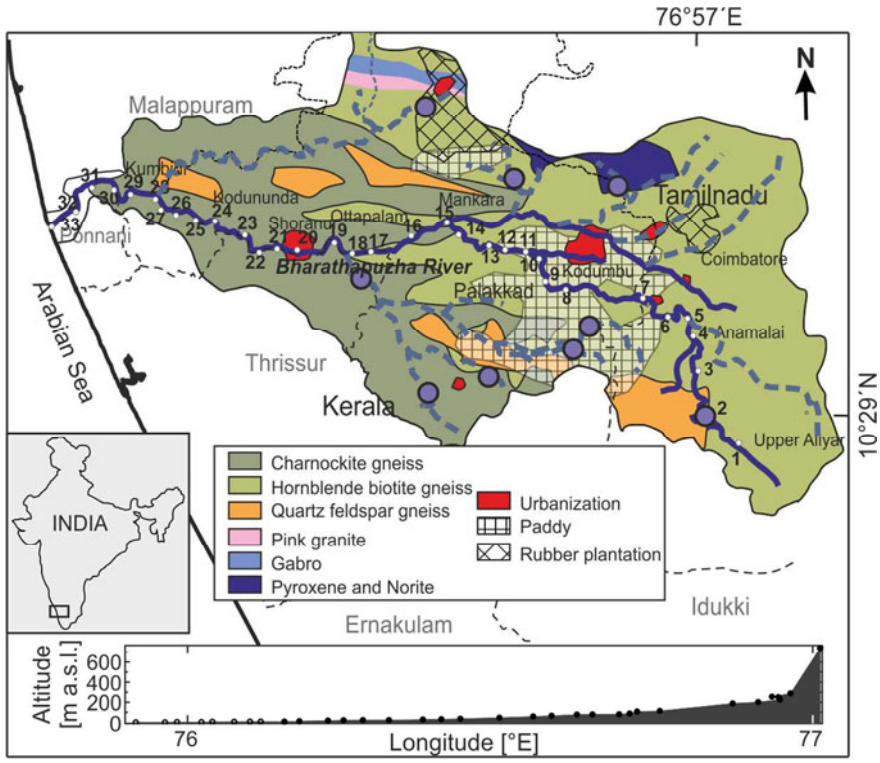

Fig. 1. Map of the area, Kerala state. Sediments were collected from 33 sites in the main channel along the Bharathapuzha River. Main geology and land uses are included. The basin boundary, main streams and dams (circles) are displayed. Altitude data for each site are shown in the bottom chart.

dams constructed across this river: seven in Kerala (Walayar, Malampuzha, Chulliyar, Nenmara, Pothundi, Mangalam and Cheerakuzhi) and two in Tamil Nadu (Thirumurthi and Aliyar). Malampuzha is the largest dam. With a drainage area of 6186 km^2, Bharathapuzha watershed is one of the largest river basins in Kerala, useful to irrigate an area of 773 km^2. Two thirds of the total drainage area (4400 km^2), are in Kerala and the remaining 1786 km^2 are in Tamil Nadu.

The Bharathapuzha River flows through three major physiographic regions, the highlands (> 75 m a.s.l.), the midlands (8–75 m a.s.l.) and the lowlands (< 8 m a.s.l.), which constitutes highly varied geological formations (*Sreela, 2009*, Fig. 1). These physiographic regions along the river were estimated by the Centre for Water Resources Development and Management (CWRDM, *Basak et al., 1995*). Various physiographic characteristics of a drainage basin such as size, length of the tributaries, drainage density, and slope can be correlated with hydrological phenomena (*Magesh et al., 2013*). As sampling was made along the main channel, downstream order and basin's size increase as other morphological variables do.

The geology of the study area is summarised in Fig. 1. The area is characterised by Archaean crystalline formation (gneiss, schist, charnockite), Tertiary formations, sub-recent laterite and recent riverine alluvium (*Sakthimurugan, 2007*). A major part of the study area is underlined by Precambrian metamorphic rocks. The highlands are represented mostly by hornblende-biotite gneiss over quartz feldspar gneiss, whereas in the midlands outcrop, this was charnockite and charnockite gneiss. This region also includes some parts of quartz-feldspar gneiss, biotite-hornblende gneiss with, pink granite, schist and quartz syenite. Acidic rocks like granulite pyroxene, norite and basic rocks like gabbro and dolerite are intruded at many places. The latter, together with pyroxene granulites, are restricted to the northern part of the basin. In the lowlands, Charnockite gneiss is overlain by Miocene to recent sedimentary deposits like alluvium and coastal sands (*Sreela, 2009*; *Sreela et al., 2012*; *Magesh et al., 2013*; *Nikhil Raj and Azeez, 2012*). In Fig. 1, main land uses are also shown: urbanisation, paddy and rubber plantation (*Sreela, 2009*).

The study area has a tropical humid climate with a humidity range of 80–96%, and an annual temperature between 22.7 and 32.5°C. The average rainfall of this area is ~2800 mm. Every year, 4000 million m^3 of water flows from the Bharathapuzha River to the Arabian Sea.

This river is the most important source of drinking water and is commonly used for agriculture and domestic purposes. Domestic and agricultural wastes from the population living along the river pollute it to a greater extent. The sediments of this river are extensively used for the construction of buildings by the people of Coimbatore, Palakkad and Malappuram districts. In recent years, the basin has been facing severe water scarcity and drought, especially due to anthropogenic pressures, such as unsustainable exploitation of natural resources and intrusion of the river course and basin areas by dams and irrigation projects, cultivation and extensive mining of sand and clay (*Raj and Azeez, 2009*).

3. MATERIALS AND METHODS

3.1. Sampling

Bed sediment samples were collected in the main channel along the Bharathapuzha River region starting from Upper Aliyar (foot of Anamalai Hills) in Tamilnadu State and ending in Ponnani (Arabian Sea) in Kerala State. Sampling was made during the dry season between March 2012 and June 2012 at a water depth of ~5 cm and ~30 cm from the river coast. Thirty-three bed sediment samples were collected from the bottom of the main channel of the river in polyethylene bags and then air-dried on aluminium trays at room temperature in open air. Sampling site locations are separated approximately by a distance of 4–5 km from each other, and are given in Supplementary data.

3.2. Magnetic measurements

Each sample was sub sampled for magnetic studies using plastic containers (2.3 cm^3). Dry samples were sieved (2 mm) to remove the gravel fraction, and then they were packed, weighed, and labelled. After that, all of the samples were fixed using sodium silicate to prevent unwanted movements in studies of remanence magnetisation. Each sample was impregnated and saturated with a sodium silicate (diluted at 5%wt) solution, and dried at room temperature until its consolidation.

Magnetic measurements were carried out in the laboratory of the CIFICEN (Tandil, Argentina). Magnetic susceptibility measurements and remanence measurements were carried out, in particular, anhysteretic remanent magnetisation (*ARM*) and isothermal remanent magnetisation acquisition (IRM).

Magnetic susceptibility measurements were performed using a magnetic susceptibility meter MS2, Bartington Instruments Ltd., linked to MS2B dual frequency sensor (0.47 and 4.7 kHz). The volume-specific magnetic susceptibility (κ), its frequency-dependence $\kappa_{\mathrm{FD\%}} = \left(\kappa_{0.47} - \kappa_{4.7}\right)/\kappa_{0.47}$ (in %) and mass-specific magnetic susceptibility $\chi = \kappa/\rho$, where ρ is the bulk density, were computed.

The *ARM* was imparted using a partial *ARM* (pARM) device attached to a shielded demagnetiser (Molspin Ltd.), superimposing a DC bias field of 10, 60 and 90 μT to an alternating field (AF) of 100 mT, and an AF decay rate of 17 μT per cycle. The remanent magnetisation was measured by a spinner fluxgate magnetometer Minispin (Molspin Ltd.). Anhysteretic susceptibility (κ_{ARM}) was estimated using linear regression for *ARM* acquired at different DC bias fields (7.96, 47.75 and 71.58 A/m). Related parameters, such as χ_{ARM}, King's plot (χ_{ARM} versus χ, *King et al., 1982*) and the $\kappa_{\mathrm{ARM}}/\kappa$ ratio, were also calculated.

The IRM studies were carried out using a pulse magnetiser model IM-10-30 (ASC Scientific). Each sample was magnetised by exposing it to growing stepwise DC fields: 27 forward steps from 4.3 mT to 2470 mT. The remanent magnetisation after each step was measured using the above-mentioned magnetometer, Minispin. In these measurements, IRM acquisition curves and saturation remanent magnetization *SIRM* were found using forward DC fields. Remanent coercivity (H_{cr}, the backfield required to remove the *SIRM*) and *S*-ratio ($S = -IRM_{-300}/SIRM$, where IRM_{-300} is IRM acquired after the application

of backfield of 300 mT), were also calculated from IRM measurements, using backfield once the *SIRM* was reached.

3.3. Chemical analysis

Nine selected sediment samples along the main channel were studied for quantitative chemical analysis. Each sample was sub-sampled for this study and oven-dried at 110°C, passed through a 2 mm mesh sieve and ground to fine powder using an agate mortar. Major elements (Si, Al, Mn, Mg, Na, Ca, K, Ti and P) were determined by XRF analysis (Pressed Pallet Method) by using a computerised sequential X-ray Fluorescence Spectrometer (Philips PW1480) containing a Rh X-ray tube fitted to flow proportional counter & scintillation counter using standard reference materials like silicate rocks, cements and limestone.

For trace element analysis, sediment samples were digested using the standard aqua-regia digestion method according to ISO 11466 standard method (*Parizanganeh et al., 2012*). Three g of sediment was accurately weighed and placed in a 100 ml round-bottomed flask and made to react with 21 ml of concentrated HCL and 7 ml of concentrated HNO3 for 16 h (overnight) at room temperature. The mixture was manually shaken, covered with a watch glass and kept at room temperature for 16 h (overnight). A Dimroth type reflux condenser was placed on top of the flask and gently heated to boiling for 2 h, as performed by *Yafa and Farmer (2006)*. After cooling, the condenser was rinsed with 25 ml of water (milli-Q) and collected in the flask. The mixture was filtered through Whatman No. 42 filter paper after removing the condenser. The residue and the filter were rinsed 3-times with 5 ml of water. The solution was transferred into a polyethylene volumetric flask and diluted with milli-Q water to 100 ml. The concentrations of trace metals (Cr, Cu, Ni, Pb, Zn, Fe and Cd) were measured using an Inductively Coupled Optical Emission Spectrometer (Perkin Elmer Optima 5300 DV). Reagent blanks, standard reference soil samples, and internal control samples were also analysed in order to monitor analytical accuracy and precision (*Tume et al., 2006*).

3.4. Radionuclide data

Thirty-three sediment samples were sub-sampled and prepared according to the protocol and procedures detailed by *Krishnamoorthy et al. (2014)*. ^{226}Ra, ^{232}Th and ^{40}K activity concentrations in sediment samples were measured using a coaxial n-type high purity germanium (HPGe) detector based on high resolution gamma spectrometry system (EG&G, ORTEC, Oak Ridge, USA). The relative efficiency of the detector is 20%, and it has a resolution of 2.0 keV at 1332 keV. The output of the detector was analysed using a 4K multichannel analyser system connected to a PC and an ADC for data acquisition.

3.5. Microscopy

Magnetic extracts were examined by scanning electron microscopy (SEM), using a JEOL JSM-6460LV microscope. The magnetic extraction for representative samples (belonging to the highland, midland and lowland areas) was performed using a hand magnet. Before SEM observation, each specimen was prepared with a thin coating of Au/Pd. The composition of 22 individual grains was analysed by X-ray energy dispersive spectroscopy (EDS) investigations. The system used was an EDAX Genesis XM4 - Sys

60, equipped with Multichannel Analyser EDAX mod EDAM IV, Sapphire Si(Li) detector and Be Super Ultra-Thin Window running EDAX Genesis version 5.11 software.

3.6. Statistical techniques

Descriptive statistics and Pearson's correlation coefficients for all variables and data were studied as a first step. Multivariate statistical analysis, in the form of principal component analysis (PCA), was performed using the R free software (R version 2.15.0, *http://www.r-project.org/*). The data set included radioactivity variables (for $n = 33$ samples, reported by *Krishnamoorthy et al., 2014*), magnetic variables (for $n = 33$ samples) and chemical variables (for $n = 9$ samples).

4. RESULTS AND DISCUSSION

4.1. Magnetic carriers

The results of magnetic concentration (χ, *ARM* and *SIRM*), mineralogy (H_{cr}, *S*-ratio and $SIRM/\chi$) and grain-size ($\kappa_{FD\%}$, κ_{ARM}/κ, $SIRM/\chi$ and $ARM/SIRM$) dependent parameters are displayed in Supplementary Data.

Values of χ, *ARM* and *SIRM* vary widely along the river, decreasing by a factor of 60 from the uppermost catchments (2160.6×10^{-8} m^3kg^{-1}, 1131.5×10^{-6} Am^2kg^{-1} and

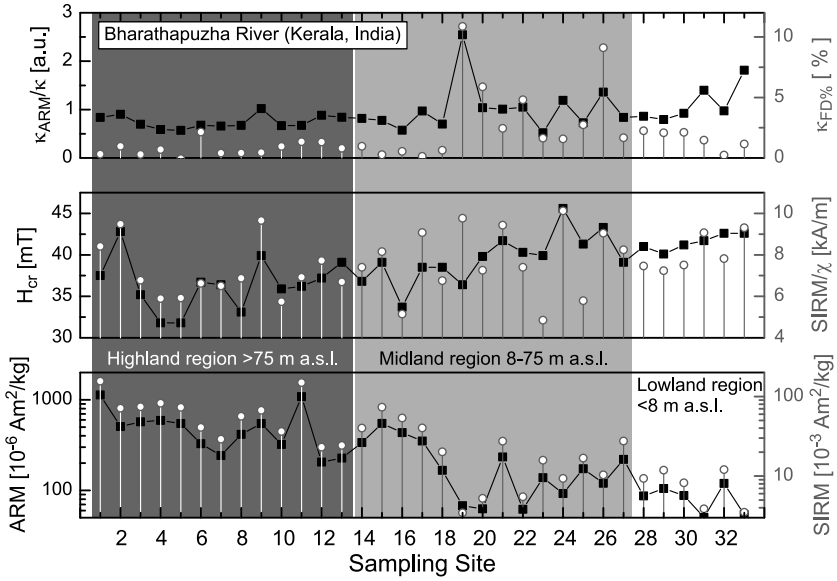

Fig. 2. Spatial distribution of magnetic parameters along the Bharathapuzha River. Three physiographic regions are indicated. Magnetic concentration-dependent parameters (*ARM* and *SIRM*), magnetic mineralogy-dependent parameters (H_{cr} and $SIRM/\chi$) and magnetic grain size-dependent parameters (κ_{ARM}/κ and $\kappa_{FD\%}$).

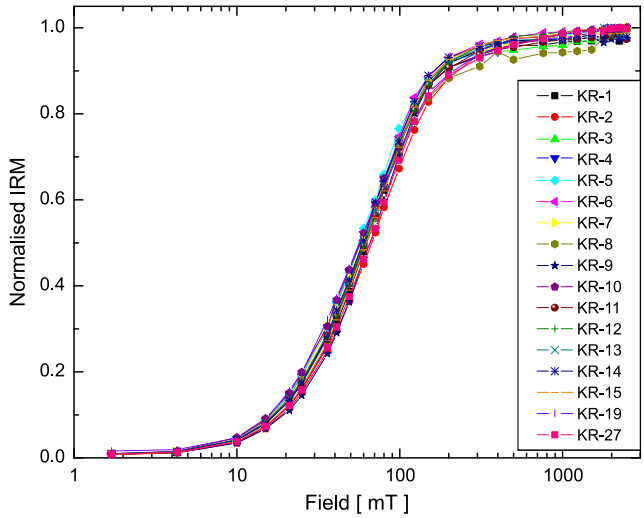

Fig. 3. Curves of acquisition of remanent magnetization for selected samples.

155.4×10^{-3} Am^2kg^{-1}) to the mouth (35.4×10^{-8} m^3kg^{-1}, 50.4×10^{-6} Am^2kg^{-1} and 3.5×10^{-3} Am^2kg^{-1}, see *ARM* and *SIRM* values in Fig. 2). Although magnetic susceptibility is a dia, para, antiferro and ferrimagnetic concentration-dependent parameter, in general, a very low content of magnetite-like (ferrimagnetic) minerals controls the magnetic signal in sediments.

The IRM acquisition measurements show the dominance of ferrimagnetic minerals (Fig. 3). Most of the curves reach values close (91–96%) to their saturation at a field of 300 mT (saturation characteristic field for ferrimagnetic minerals); hence, a contribution of high coercivity minerals is not evident from these measurements.

Measurements of remanent magnetisation and their related magnetic parameters (H_{cr} and *S*-ratio) suggest that the magnetic signal is controlled by a ferrimagnetic phase. The *S*-ratio values (between 0.811 and 0.998) clearly show the predominance of low-coercivity minerals (*S*-ratio close to 1) over high-coercivity minerals (*S*-ratio close to –1).

On the other hand, the values of H_{cr} range from 31.8 to 45.6 mT (Supplementary Data), which are in agreement with characteristic values of (titano)magnetite (*Peters and Dekkers, 2003*). The H_{cr} values range narrowly indicating a similar magnetic mineralogy for these sediment samples. However, even within this narrow range, higher H_{cr} values may be due to an additional contribution of high-coercivity and/or finer ferrimagnetic grains.

The magnetic minerals were observed by SEM in three magnetic extracts from Sites 1 (highlands), 21 (midlands) and 29 (lowlands, see Fig. 4). Their composition was determined by EDS, showing the presence of titanomagnetite minerals with variable contents of Fe, Ti and O. Although the observed Fe-rich particles (up to 51 wt%) show an important Ti contribution (up to 26 wt%), lower Fe/Ti-ratio values are observed in particles from highlands (~1.9) and midlands (~1.3), than in lowlands (~5.4).

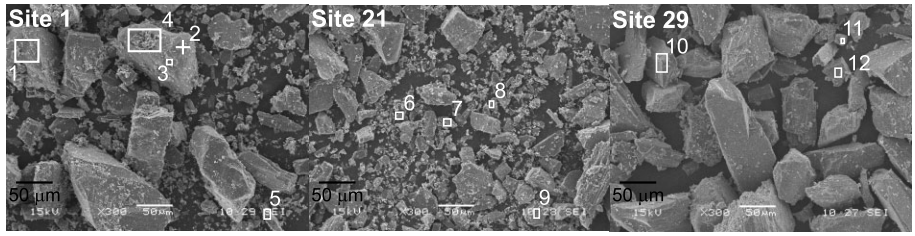

Fig. 4. SEM images of magnetic extracts of sediments from the highlands (Site 1), midlands (Site 21) and lowlands (Site 29). The composition of irregular particles was determined by EDS and is indicated with the numbers 1–12. All of the indicated particles are composed of variable contents of Fe, Ti and O (titanomagnetite). A higher abundance of Ca was found in Site 1 (e.g., #4 and #5) than in Site 29 (e.g., #10). K and P were detected in #4 and #5, respectively; and Mn in #5, #7 and 9. Al, Si and Mg were detected in most of the sites (e.g., #3, #4, #5, #10 and #11).

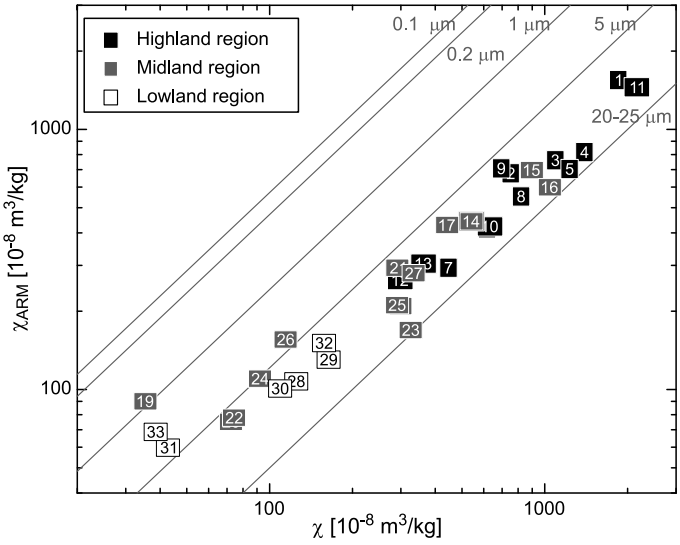

Fig. 5. King's Plot (anhysteretic magnetic susceptibility χ_{ARM} versus mass-specific susceptibility χ) for all samples. Most of the samples are between 5 and 20 μm, samples with higher magnetic concentration-dependent parameters trend to coarser magnetic grain sizes. Numbers represent the sampling sites.

Values of χ_{ARM} and χ for all samples are displayed in the King's plot (Fig. 5). In this biplot, it is possible to observe magnetic grain sizes above 1 μm, most of them coarser grains, between 5 and 20 μm. Higher values of χ coincide with lower values of κ_{ARM}/κ and $ARM/SIRM$ (Fig. 6, negative significant correlations with χ, *ARM* and *SIRM*, e.g., Pearson's coefficient between −0.395 and −0.585, Table 1), and vice versa; hence, higher

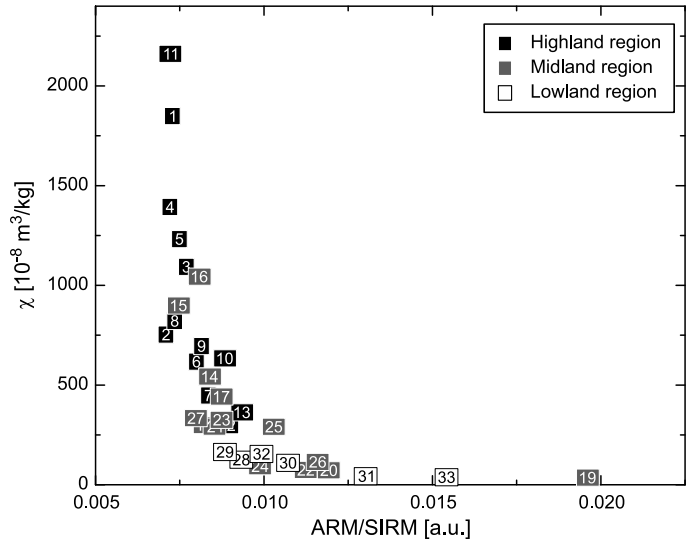

Fig. 6. Biplot using magnetic grain-size (ratio of anhysteretic and saturation remanence, $ARM/SIRM$) and concentration-dependent parameter (mass-specific susceptibility χ). Numbers represent the sampling sites.

(lower) values of magnetic concentration are accompanied by the presence of coarser (finer) magnetic grains.

Values of $SIRM/\chi$ from 4.8 to 10.1 kA/m belong to the range of magnetite, whereas higher values are interpreted as finer magnetic grain sizes abundance. This interpretation, according to *Peters and Dekkers (2003)*, is based on the fact that magnetite grains are bigger than 1 μm. This is also supported by the significant positive correlation between $SIRM/\chi$ and κ_{ARM}/κ ($R = 0.695$, $p = 7.2 \times 10^{-6}$).

The presence of ultrafine (< 0.03 μm) superparamagnetic minerals (SP) can be observed from the $\kappa_{FD\%}$. In Supplementary Data, it is possible to note some high values of $\kappa_{FD\%}$ (4.8–10.9%) that are indicative of the presence and dominance (the highest values) of SP grains (*Dearing et al., 1996*; *Dearing, 1999*). This parameter correlates statistically with sensible grain size-dependent parameters κ_{ARM}/κ and $ARM/SIRM$ ($R = 0.680$, $p = 1.3 \times 10^{-5}$ and $R = 0.722$, $p = 2.1 \times 10^{-6}$; respectively).

4.2. Spatial distribution

The concentration-dependent magnetic parameters display variations along the river. Values of *ARM* and *SIRM* show clear differences between the physiographic regions, being higher at the highland region (Sites 1–13) and at some sites from the midland region (see Fig. 2). The lowland region has the lowest concentration-dependent magnetic parameters, being about 5–7-fold lower than the highland region. For example, mean *SIRM* values decrease from the highland region (67.9×10^{-3} Am^2kg^{-1}) to the lowland

Table 1. Pearson's correlation coefficients between magnetic parameters and radioactivity data (33 samples) and between magnetic parameters and elemental composition data (9 samples) for the sediment samples from the Bharathapuzha River. χ: mass-specific susceptibility, *ARM*: anhysteretic remanence, *SIRM*: saturation remanence, $\kappa_{FD\%}$: frequency-dependent susceptibility, H_{cr}: coercivity of remanence. See text for definition of the parameters.

	χ	*ARM*	*SIRM*	$\kappa_{FD\%}$	κ_{ARM}/κ	$ARM/SIRM$		H_{cr}
ARM	0.970[a]							
SIRM	0.972[a]	0.998[a]						
$\kappa_{FD\%}$	–0.412[b]	–0.409[b]	–0.410[b]					
κ_{ARM}/κ	–0.467[a]	–0.395[b]	–0.397[b]	0.680[a]				
$ARM/SIRM$	–0.585[a]	–0.573[a]	–0.577[a]	0.722[a]	0.916[a]			
$SIRM/\chi$					0.695[a]	0.398[b]		
H_{cr}	–0.620[a]	–0.497[a]	–0.491[a]		0.374[b]		0.589[a]	
S-ratio	0.462[a]	0.462[a]	0.452[a]					–0.559[a]
Ni					–0.671[b]	–0.754[b]		
Zn				–0.722[b]				
Si							0.681[b]	0.849[a]
Fe	0.693[b]	0.705[b]	0.696[b]	–0.697[b]				
Ca	0.809[a]	0.715[b]	0.733[b]					
P	0.877[a]	0.911[a]	0.910[a]					
^{226}Ra	–0.406[b]	–0.443[a]	–0.437[a]	0.369[b]		0.394[b]		0.397[b]
^{40}K	0.526[a]	0.504[a]	0.513[a]			–0.372[b]		–0.416[b]

a significance at the 0.01 level
b significance at the 0.05 level

region ($9.4 \times 10^{-3} Am^2kg^{-1}$, Table 2). On the other hand, differences between these 3 regions were analysed using a non-parametric one-way analysis of variance: the Kruskal-Wallis (KW) test. There are statistical differences ($p < 0.05$) between median values of χ, *ARM* and *SIRM* of the highland region and midland, lowland regions.

Four out of the 33 sites evidence the presence of SP grains; in particular, in midland sites (19, 20, 22 and 26), and in lowland region samples, relatively high values of $\kappa_{FD\%}$ are also observed (Fig. 2). Other sites, from Upper Aliyar to Ponnani, have very low mean values that increase from the highland to the lowland region.

Although there are clear differences between regions from the ratios κ_{ARM}/κ and $ARM/SIRM$ (Table 2), samples from highland and lowland regions are grouped on the left and right (respectively) in Fig. 6. In addition, the KW test yielded significant statistical differences ($p < 0.05$) of median $\kappa_{FD\%}$, κ_{ARM}/κ and $ARM/SIRM$ values between the highland and other regions (midland and lowland). Such differences indicate the predominance of coarser magnetic grains in the highland region than the others. This could be attributed to grain size sorting during sediment transport, although it is obliterated by dams, so this generalisation is not completely possible in this scenario.

Table 2. Mean values and coefficient of variation $CV = St.Dev./mean$ of magnetic parameters, activity concentration of radionuclides and elemental concentration for Bharathapuzha River (India). χ: mass-specific susceptibility, *ARM*: anhysteretic remanence, *SIRM*: saturation remanence, $\kappa_{FD\%}$: frequency-dependent susceptibility, H_{cr}: coercivity of remanence. See text for definition of the parameters.

	All Regions (33 samples)		Highland > 75 m a.s.l. (13 samples)		Midland 8–75 m a.s.l. (13 samples)		Lowland < 8 m a.s.l. (7 samples)	
	Mean	*CV* [%]	Mean	*CV* [%]	Mean	*CV* [%]	Mean	*CV* [%]
χ [10^{-8} m^3 kg^{-1}]	540.6	*98.1*	950.2	*60.2*	351.1	*90.4*	131.8	*65.0*
ARM [10^{-6} Am^2 kg^{-1}]	309.7	*87.2*	516.2	*57.2*	217.9	*71.7*	96.7	*43.4*
SIRM [10^{-3} Am^2 kg^{-1}]	38.8	*98.6*	67.9	*62.9*	25.5	*83.2*	9.4	*50.5*
$\kappa_{FD\%}$ [%]	1.9	*129.4*	0.8	*75.9*	3.1	*112.7*	1.7	*48.5*
κ_{ARM}/κ	0.93	*41.8*	0.75	*15.9*	1.02	*49.4*	1.07	*36.4*
$ARM/SIRM$	0.009	*28.9*	0.008	*10.7*	0.010	*33.5*	0.011	*20.3*
$SIRM/\chi$	7.6	*18.9*	7.2	*18.1*	7.9	*21.0*	7.7	*15.3*
Hcr [mT]	38.7	*8.7*	36.4	*8.6*	39.4	*7.7*	41.5	*2.2*
S-ratio [a.u.]	0.909	*4.4*	0.923	*4.8*	0.908	*4.2*	0.883	*3.0*
^{226}Ra [Bq kg^{-1}]	41.9	*26.0*	34.1	*18.3*	43.4	*18.9*	53.4	*21.2*
^{232}Th [Bq kg^{-1}]	54.9	*35.7*	50.2	*37.1*	50.3	*28.1*	72.0	*31.5*
^{40}K [Bq kg^{-1}]	477.8	*40.9*	644.94	*32.2*	337.3	*20.7*	428.1	*9.5*
Cr [ppm]	11.96	*25.4*	12.63	*23.0*	13.60	*35.1*	9.96	*17.8*
Cu [ppm]	5.04	*44.4*	5.48	*55.1*	4.81	*46.1*	4.60	*38.6*
Ni [ppm]	2.78	*26.1*	3.23	*18.9*	2.74	*12.7*	2.21	*34.7*
Pb [ppm]	13.27	*26.0*	14.86	*34.5*	11.91	*13.7*	12.59	*22.4*
Zn [ppm]	40.07	*14.4*	45.30	*8.5*	34.97	*10.9*	36.50	*5.6*
Fe [ppm]	5023	*17.3*	5475	*14.0*	5293	*22.4*	4240	*4.3*
Si [ppm]	272831	*4.9*	266041	*6.8*	282532	*2.1*	275417	*1.8*
Al [ppm]	62128	*5.1*	62553	*6.2*	63574	*6.9*	60597	*2.5*
Mn [ppm]	329	*32.2*	343	*31.4*	412	*25.1*	257	*32.9*
Mg [ppm]	813	*18.8*	825	*20.9*	960	*8.8*	700	*9.9*
Ca [ppm]	17335	*20.9*	18697	*26.6*	18125	*11.4*	14991	*5.3*
Na [ppm]	16987	*1.7*	17020	*2.4*	17057	*1.5*	16897	*0.7*
K [ppm]	12293	*16.5*	13093	*18.1*	12575	*20.1*	11039	*9.1*
Ti [ppm]	5307	*44.3*	5655	*53.3*	6510	*20.2*	4040	*46.4*
P [ppm]	206.361	*43.3*	265.478	*32.0*	222.87	*25.0*	116.533	*11.5*

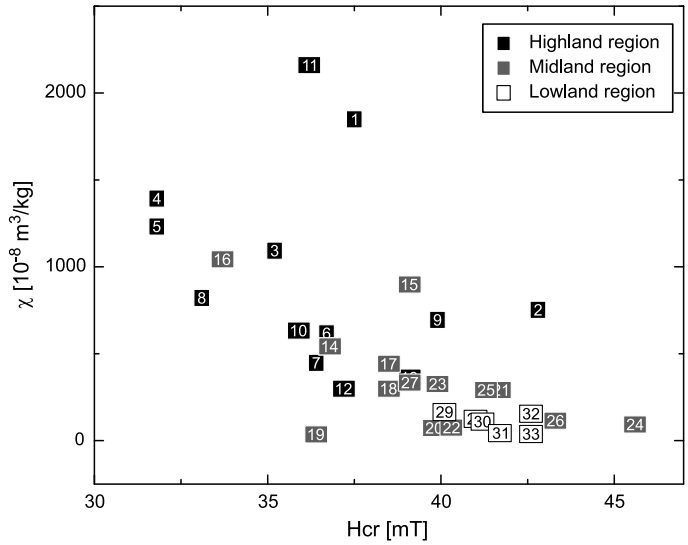

Fig. 7. Biplot of coercivity of remanence (H_{cr}), sensitive to magnetic mineralogy, and mass-specific susceptibility (χ), reflecting concentration of magnetic minerals. Numbers represent the sampling sites.

The magnetic mineralogy-dependent parameters show a slightly increasing (decreasing) trend of H_{cr} (S-ratio) mean values towards the river mouth (Table 2 and Fig. 7). This indicates that there are no important differences in the magnetic mineralogy along the river, but slight differences between regions. From these results, higher coercivity magnetic grains seem to be expected in the lowland region. According to the KW test, the highland region and the other regions (midland and lowland) have statistical differences ($p < 0.05$) between medians for parameters H_{cr} and S-ratio.

4.3. Major and trace elements and natural radionuclides

The element concentrations of Bharathapuzha River's bed sediments were normalised to the upper continental crust (UCC, *McLennan, 2001*) and they are shown in a spider diagram (Fig. 8). The normalisation was performed to show the enrichments or depletion of chemical elements related to a pattern of reference. Samples were divided following previous physiographic criteria (*Raj and Azeez, 2009*), and the mean values (excluding the Site 1) are presented, as well as the maximum (Site 1) and minimum values for the basin. Because there are no geochemical data of the exposed rocks of the study area, reference samples of granite and gneisses rock, and sediments generated from these acidic environments (*Lecomte, 2006*; *Rapela et al., 1982*; *Guereschi and Baldo, 1993*) are included for geochemical pattern comparison.

Figure 8 shows that the sediments of the study area present a depleted chemical concentration in most elements, except Ti (which was also observed by EDS). These concentration differences can be attributed to higher chemical weathering due to climate. Reference examples present signatures that are more similar to the UCC geochemical

pattern (i.e. UCC line equal 1). Elements behind UCC concentration are interpreted as weathered from minerals due to their chemical instability. On the other hand, elements that present a higher concentration than UCC should be due to additional sources. In Bharathapuzha sediments, the only element which appears with higher concentrations than the upper continental crusts is Ti. This element is abundant in the UCC; therefore, its relatively increased concentration may be attributed to pollution sources. In Fig. 8, there are some other aspects to take into account. The Upper Aliyar sampling site (Site 1, the uppermost catchment) presents the highest chemical concentrations (i.e., Al, Fe, Mg, Na, K, Ti and P) that are also noted in magnetic extracts by EDS studies (see Fig. 4). These relatively high values should be probably to their presence in accessory minerals in quarzo-feldespatic gneisses, as well as contamination by intense farm activity (Fig. 1). It is also observed that there are some elements whose concentrations decrease with height, from the upper to the lower basin (Ti, Fe, Ni, Zn, P, K and Ca, Table 2). The latter was also observed by EDS (Fig. 4) where higher contents of Ti and Ca were found in Site 1, as well as the presence of particles containing K, P and Mn. Some of the mentioned elements are common constituents of agrochemical additives, such as pesticides and chemical fertilisers, used in agricultural activities. Moreover, most of these elements are not easily weathered, so they should increase their relative concentration downstream. As reported by *Chauhan et al. (2013)*, in different fertiliser samples from the Indian markets and industries, these fertilisers (e.g., potash fertiliser, nitrogen phosphorous potassium, zinc sulphate, organic fertiliser, etc.) contain enhanced concentrations of natural radionuclides

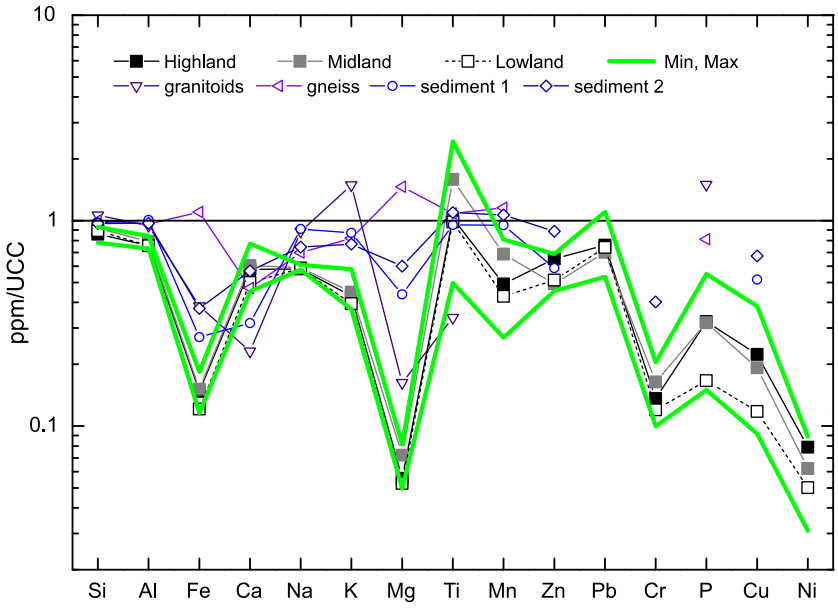

Fig. 8. UCC-normalised values of major and trace element for nine selected sites from highland (Sites 1, 5, 9 and 13), midland (Sites 17 and 21) and lowland (Sites 25, 29 and 33) regions are shown. Normalisation was performed using the upper continental crust (UCC, *McLennan, 2001*). Mean values for acid rocks (granitoid and gneiss) and sediments are also showed for reference.

coming from phosphate rocks. They also reported the presence of P_2O_5, K_2O, SiO_2, Al_2O_3, SO_3, Cl, and Fe_2O_3 as major components (from a total of 15), as well as the presence of fluorapatite, hydroxylapatite, chlorapatite and iron oxides.

In this high region, farm and agricultural activities are intensive (*Kannan and Joseph, 2009*). The use of pesticide on soils can also lead to a reduction (by dissolution) of Fe-bearing minerals and SP grains, as reported by *Agustine et al. (2013)*. The non-organic fertilisers mainly contain phosphate, nitrate, ammonium and potassium salts, and are also considered to be a potential source of heavy metals and natural radionuclides (*Akhtar et al., 2005*; *Savci, 2012*). Pollution of paddy soils by potentially toxic metals mainly due to phosphate fertiliser applications has been reported, especially in areas with economic development. For example, *Chandrajith et al. (2010)* analysed the relation between toxic metals with fertilisers and agro-chemicals in rice field soils. They (and also references therein) concluded that the chemical concentration of toxic metals is a result of both mineralogical and anthropogenic processes.

On the other hand, some elements exhibit their maximum concentration at the middle basin (Ti, Cr, Cu, Fe, Mn, Mg, Si and Al) after crossing urbanised areas (Site 17 and Site 21). In the river mouth (Site 33), a concentration increase for Fe, Mn and Ti was also observed, probably due to adverse influences produced by urban areas.

Bharathapuzha river sediments, as explained above, have variable behaviour related to Fe, Ca and Ti concentrations rather than other sediments, probably due to anthropogenic contamination (urban and agricultural activities). This result is consistent with the multivariate analysis, which related some of these parameters with χ, *ARM* and *SIRM* variables and is also consistent with the SEM-EDS analysis.

The activity concentrations of natural radionuclides are detailed in Supplementary Data. In general, the mean values of ^{226}Ra, ^{232}Th and ^{40}K (41.9, 54.9 and 477.8 Bqkg^{-1}, respectively) are higher than the International (35, 30 and 400 Bqkg^{-1}, respectively) and Indian recommended values (*UNSCEAR, 2000*). From Table 2, it is possible to observe a clear variation of ^{226}Ra, ^{232}Th and ^{40}K mean values between the highland (34.1 50.2 and 644.9 Bqkg^{-1}, respectively) and lowland (53.4, 72.0 and 428.1 Bqkg^{-1}, respectively) regions. These differences between regions were also found using the Kruskal-Wallis test. There are statistical differences ($p < 0.05$) between median values of activity concentration. For, ^{232}Th, there are differences between the lowland region and the other regions (highland and midland); on the other hand, for ^{226}Ra and ^{40}K, there are differences between the highland region and other regions (midland and lowland). These results indicate that sediments with different activity concentrations of ^{226}Ra, ^{232}Th and ^{40}K can be collected along the Bharathapuzha River from different physiographic regions. The higher concentration of ^{40}K may be due to the use of chemical fertiliser to a large extent in agriculture (*Akhtar et al., 2005*), e.g., potassium fertilisers are excessively used in agriculture activities (intense cultivation for wet and dry crops) in this area (*Kannan and Joseph, 2009*). Studies of fertilisers in several countries, including Finland (*Mustonen, 1985*), Italy (*Righi et al., 2005*), Saudi Arabia (*Alharbi, 2013*), Nigeria (*Jibiril and Fasae, 2012*) and India (*Chauhan et al., 2013*), have reported the enhanced concentration of natural radionuclides. Radionuclides, together with some other heavy metals, are the primary toxic pollutants for phosphate fertilisers. In fact, these are

dispersed in significant amounts via fertilisers. Therefore, it is necessary to pay attention to the use of fertilisers in agriculture and its environmental impact (*Roselli et al., 2010*). *Chandrajith et al. (2010)* found a high correlation between radionuclides and fertilisers and agro-chemicals in rice field soils. They demonstrated that the continued application of phosphate fertilisers could increase ^{40}K contents.

4.4. Relationships between magnetic, chemical and radionuclide variables

The statistical multivariate analyses were applied in order to achieve two aims: (1) identify the relationship between magnetic, radioactivity and elemental variables; and (2) data classification according to different variables and their adverse influence.

As observed in Table 1, the bivariate analysis shows significant correlations between variables. Among the magnetic variables, it is interesting to note that concentration-dependent variables, i.e.: χ, *ARM* and *SIRM*, correlate with various non-magnetic variables; in particular, significant correlations are observed with Fe (R = 0.693–0.705 at the 0.05 level), and at the 0.01 level with Ca (R = 0.715–0.809), P (R = 0.877–0.911), ^{226}Ra and ^{40}K (R = 0.504–0.526).

The PCA uses the correlation matrix to represent variables in the coordinate plane of principal components (PC). The data matrix was standardised with a column range, and then a correlation matrix was used. The PCA was carried out to study, in a multivariate way, the one-to-one relationships between the variables detailed earlier. The variables and samples are represented in Fig. 9a,b, regarding magnetic and radioactivity variables (M-R variables, Fig. 9a), as well as magnetic and elemental variables (M-E variables, Fig. 9b).

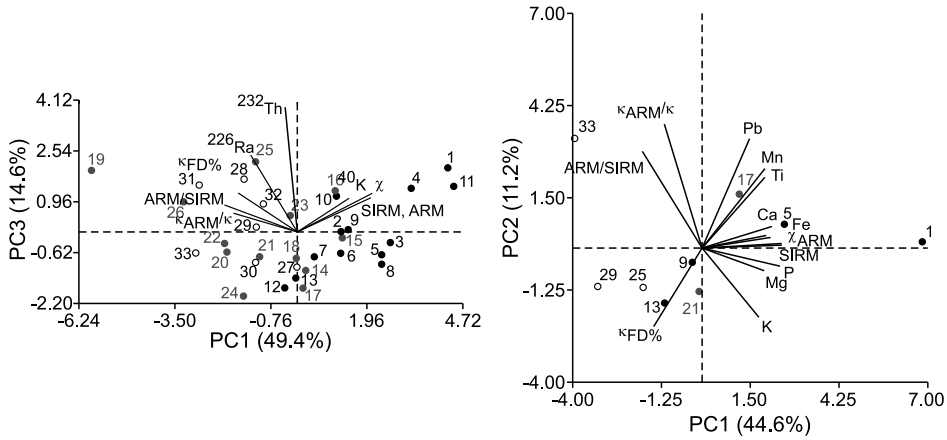

Fig. 9. Principal component analysis (PCA) for the highland (●), midland (●) and lowland (○) regions, using different variables: **a)** magnetic and radioactivity variables (33 samples); **b)** magnetic and chemical variables (9 samples). The first principal components (PC1 and PC3/PC2) are shown. The first PCs accounted for 64% for M-R and M-E of the total variance. Different groupings of variables and individuals (belonging to different regions) are observed.

The "average" samples are located close to the PC's origin; on the contrary, other samples (Sites 1, 4, 11, 19, 26 and 33 in Fig. 9a; Sites 1, 5, 29 and 33 in Fig. 9b) show a distinctive behaviour. Samples from the highland region are well grouped and located on the right sector; on the contrary, samples from the lowland region are grouped on the left. Such behaviour is consistent with high (low) magnetic concentration, low (high) coercivity minerals and coarse (fine) magnetic grains. The samples from the midland region show an in-between behaviour, this is particularly observed from the random distribution of these samples around the PC's origin.

Some variables are grouped and show a good correlation between them. On the one hand, for magnetic and radioactivity variables, χ-*ARM*-*SIRM* are positively correlated with ^{40}K and negatively with ^{232}Th and ^{226}Ra. The latter results support the use of χ, *ARM*, *SIRM* as indicators of natural radioactivity levels of ^{226}Ra, ^{232}Th and ^{40}K in Bharathapuzha River. As mentioned, some investigations have shown the correlation of radionuclide concentrations and magnetic minerals (e.g., *McCubbins et al., 2004*; *Montes et al., 2012*; *Ramasamy et al., 2014*). *Suresh et al. (2011)* found that χ is positively correlated with the concentration of ^{232}Th ($R = 0.603$), and the concentration of ^{40}K ($R = 0.483$), yet negatively correlated with the concentration of ^{238}U.

On the other hand, for magnetic and elemental variables, χ-*ARM*-*SIRM* are positively correlated with Cr-Fe-Ca-P; $\kappa_{FD\%}$- $ARM/SIRM$ -H_{cr} are negatively correlated with Zn-Ni-K and directly with Si. Such results are in agreement with the existence of relationships between variables from the correlation analysis.

The first two PCs accounted for the 64.0% and 64.3% of the total variance for M-R (Fig. 9a) and M-E (Fig. 9b), respectively. The PC1 showed a high factor loading of most of the variables (χ, *ARM*, *SIRM*, $\kappa_{FD\%}$, $ARM/SIRM$, ^{40}K, ^{232}Th, ^{226}Ra, Cr, Ca, P, Fe, Mn, Mg, K, and Ti). PC1 demonstrates the main contributions of χ, *ARM*, *SIRM*, ^{40}K, Cr, Fe, Ca and P with factor loadings of 0.94, 0.94, 0.94, 0.61, 0.77, 0.81, 0.82 and 0.92, respectively. This association could arise mainly as a consequence of agro-additives, which contain phosphate, nitrate, ammonium, and potassium salts, as well as heavy metals and radionuclides, as mentioned before. The PC2/3 includes the variables $\kappa_{FD\%}$, κ_{ARM}/κ, $ARM/SIRM$, ^{232}Th, ^{226}Ra, Zn, Ni, Al, Na, Pb and Si with factor loadings between 0.54 and 0.87. This result may be attributed to mineral weathering and also to urbanisation wastes.

5. CONCLUSIONS

The magnetic signal of these river bed sediments is controlled by (titano)magnetite minerals with slight variation along the river, i.e.: higher coercivity magnetic grains are expected in the lowland region.

These magnetic minerals also display variations in grain size (1–20 μm) indicating the predominance of coarser magnetic grains in the highland region. Moreover, variations in concentration-dependent magnetic parameters along the river are evident, e.g., values of χ, *ARM* and *SIRM* in the highland region are 2–3-fold higher than in the midland region, and 5–7-fold higher than in the lowland region. The spatial variation along the river can

be related to both natural and anthropogenic sources: changes in mineralogy or in land use and the influence of human activities.

The magnetic enhancement may arise as a result of pollution from intense agricultural activities in this area. This fact is supported by multivariate statistical analyses between concentration-dependent magnetic parameters and common constituents (e.g., Ca, P, Fe and ^{40}K) of agro-additives, such as chemical fertilisers from the Indian markets and industries reported by *Chauhan et al. (2013)*. The higher concentration of ^{40}K may be due to the use of potassium fertiliser to a large extent in agriculture in this area. Besides, the Bharathapuzha sediments have higher Ti concentrations than upper continental crusts and variables Fe and Ca, probably due to anthropogenic contamination.

The mean concentrations of ^{226}Ra and ^{40}K are 1.2-fold higher than the International recommended average value (*Krishnamoorthy et al., 2014*). This fact may sometimes cause health risks to humans residing in this area and using this material for construction purposes. Thus, river sediments should be collected from sites with lower values of activity concentration. In such a sense, according to the correlation between radioactivity variables and concentration-dependent magnetic parameters (e.g., χ), such magnetic parameters can be used as a no-time-consuming and low-cost method to check the adverse potential of sediments.

Acknowledgements: The authors wish to thank the Annamalai University, the UNCPBA, UNMdP, UNC and National Council for Scientific and Technological Research (CONICET) for their financial support. They also thank Mr. P. Zubeldia (Tech. CICPBA) for his help. This manuscript was greatly improved by useful suggestions and comments by Dr. Bijaksana, Dr. Petrovský and two anonymous reviewers.

Supplementary data - magnetic parameters, activity concentration of radionuclides and elemental concentration of Bharathapuzha River (India) can be obtained from http://ig.cas.cz/sites/default/files/u241/sgeg_2014_0045_chaparro_suppldata_pdf_85231.pdf.

References

Agustine E., Fitriani D., Safiuddin L.O, Tamuntuan G. and Bijaksana S., 2013. Magnetic susceptibility properties of pesticide contaminated volcanic soil. *AIP Conference Proceedings*, **1554**, 230–233.

Akhtar N., Tufail M., Ashraf M. and Mohsin Iqbal M., 2005. Measurement of environmental radioactivity for estimation of radiation exposure from saline soil of Lahore, Pakistan. *Radiat. Meas.*, **39**, 11–14.

Alharbi W.R., 2013. Natural radioactivity and dose assessment for brands of chemical and organic fertilizers used in Saudi Arabia. *J. Modern Phys*., **4**, 344–348.

Basak P., James E.J. and Nandeshwar M.D., 1995. *Water Atlas of Kerala*. CWRDM/ STEC, Calicut, India.

Beckwith P., Ellis J., Revitt D. and Oldfield F., 1986 Heavy metal and magnetic relationships for urban source sediments. *Phys. Earth Planet. Inter.*, **42**, 67–75.

Bulman R.A., Johnson T.E. and Reed A.L., 1984. An examination of new procedures for fractionation of plutonium- and americium-bearing sediments. *Sci. Tot. Environ*., **35**, 239–250.

Chandrajith R., Seneviratna S., Wickramaarachchi K., Attanayake T., Aturaliya T.N.C. and Dissanayake C.B., 2010. Natural radionuclides and trace elements in rice field soils in relation to fertilizer application: study of a chronic kidney disease area in Sri Lanka. *Environ. Earth Sci.*, **60**, 193–201.

Chaparro M.A.E, Bidegain J.C., Sinito A.M., Jurado S. and Gogorza C.S., 2004. Relevant magnetic parameters and heavy metals from relatively polluted stream-sediments - spatial distribution along a cross-city stream in Buenos Aires Province, Argentina. *Stud. Geophys. Geod.*, **48**, 615–636.

Chaparro M.A.E, Gogorza C.S.G., Chaparro M.A.E., Irurzun M.A. and Sinito A.M., 2006. Review of magnetism and pollution studies of various environments in Argentina. *Earth Planets Space*, **58**, 1411–1422.

Chaparro M.A.E., Sinito A.M., Ramasamy V., Marinelli C., Chaparro M.A.E., Mullainathan S. and Murugesan S., 2008. Magnetic measurements and pollutants of sediments from Cauvery and Palaru River, India. *Environ. Geol*., **56**, 425–437.

Chaparro M.A.E., Chaparro M.A.E., Rajkumar P., Ramasamy V. and Sinito A.M., 2011. Magnetic parameters, trace elements and multivariate statistical studies of river sediments from south eastern India: A case study from Vellar River. *Environ. Earth Sci.*, **63**, 297–310.

Chaparro M.A.E., Chaparro M.A.E. and Sinito A.M., 2012. An interval fuzzy model for magnetic monitoring: estimation of a pollution index. *Environ. Earth Sci.*, **66**, 1477–1485.

Chaparro M.A.E., Suresh G., Chaparro M.A.E., Ramasamy V. and Sinito A.M., 2013. Magnetic studies and elemental analysis of river sediments: A case study from the Ponnaiyar River (southeastern India). *Environ. Earth Sci.*, **70**, 201–213.

Chauhan P., Chauhan R.P. and Gupta M., 2013. Estimation of naturally occurring radionuclides in fertilizers using gamma spectrometry and elemental analysis by XRF and XRD techniques. *Microchem. J.*, **106**, 73–78.

Chen W., Chang A.C. and Wu L., 2007. Assessing long-term environmental risks of trace elements in phosphate fertilizers. *Ecotoxicol. Environ. Safe.*, **67**, 48–58.

De Meijer R.J., Put L.W., Bergman R., Landeweer G., Riezebos H.J., Schuiling R.D., Scholten M.J. and Veldhuizen A., 1985.. Local variation of outdoor radon concentrations in the Netherlands and physics properties of sand with enhanced natural radioactivity. *Sci. Tot. Environ.*, 45, 101–109.

De Meijer R.J., Lesscher H.M.E., Schuiling R.D. and Eldburg M.E., 1990. Estimate of the heavy mineral content in sand and its provenance by radiometric methods. *Nucl. Geophys.*, **4**, 450–460.

Dearing J., 1999. Magnetic susceptibility. In: Walden J., Oldfield F. and Smith J. (Eds), *Environmental Magnetism: a Practical Guide*. Technical Guide No. 6. Quaternary Research Association, London, U.K., 35–62.

Dearing J., Dann R., Hay K., Lees J., Loveland P., Maher B. and O'Grady K., 1996. Frequency-dependent susceptibility measurements of environmental materials. *Geophys. J. Int.*, **124**, 228–240.

Desenfant F., Petrovský E. and Rochette P., 2004. Magnetic signature of industrial pollution of stream sediments and correlation with heavy metals: case study from South France. *Water Air Soil Pollut*., **152**, 297–312.

Dunlop D.J. and Özdemir Ö., 1997. *Rock Magnetism. Fundamentals and Frontiers*. Cambridge University Press, Cambridge, U.K., 573 pp.

El-Bahi S.M., 2004. Assessment of radioactivity and radon exhalation rate in Egyptian cement. *Health Phys.*, **86**, 517–522.

El-Gamal A., Nasr S. and El-Taher A., 2007. Study of the spatial distribution of natural radioactivity in the upper Egypt Nile River sediments. *Radiat. Meas*., **42**, 457–465.

Elejalde C., Herranz M., Romero F. and Legarda F., 1996. Correlations between soil parameters and radionuclide contents in samples from Biscay (Spain). *Water Air Soil Pollut.*, **89**, 23–31.

Evans M.E. and Heller F., 2003. *Environmental Magnetism, Principles and Applications of Enviromagnetics*. Academic Press, New York, 299 pp.

Franke C., Kissel C., Robin E., Bonté P. and Lagroix F., 2009. Magnetic particle characterization in the Seine river system: Implications for the determination of natural versus anthropogenic input. *Geochem. Geophys. Geosyst.*, **10**, Q08Z05.

Guereschi A. and Baldo E., 1993. Petrología y geoquímica de las rocas metamórficas del sector centro-oriental de la Sierra de Comechingones, Córdoba. *XII Congreso Geológico Argentino y II Congreso de Exploración de Hidrocarburos*. Actas I: 1-5 (in Spanish).

Hunt A., Jones J. and Oldfield F., 1984. Magnetic measurements and heavy metals in atmospheric particulates of anthropogenic origin. *Sci. Tot. Environ.*, **33**, 129–139.

Jibiri N.N. and Fasae K.P., 2012. Activity concentrations of ^{226}Ra, ^{232}Th and ^{40}K in brands of fertilizer used in Nigeria. *Radiat. Prot. Dosim.*, **148**, 132–137.

Jordanova D.V., Hoffmann V. and Fehr T.K., 2004. Mineral magnetic characterization of anthropogenic magnetic phases in the Danube river sediments (Bulgarian part). *Earth Planet. Sci. Lett.*, **221**, 71–89.

Kannan N. and Joseph S., 2009. Quality of groundwater in the shallow aquifers of a paddy dominated agricultural river basin, Kerala, India. *World Acad. Sci. Eng. Technol.*, **3**, 1137–1155.

King J., Banerjee S.K., Marvin J. and Özdemir Ö., 1982. A comparison of different magnetic methods for determining the relative grain size of magnetite in natural materials: Some results from lake sediments. *Earth Planet. Sci. Lett*., **59**, 404–419.

Knab M., Hoffmann V., Petrovský E., Kapička A., Jordanova N. and Appel E., 2006. Surveying the anthropogenic impact of the Moldau river sediments and nearby soils using magnetic susceptibility. *Environ. Geol*., **49**, 527–535.

Krishnamoorthy N., Mullainathan S., Mehra R., Chaparro M.A.E. and Chaparro M.A.E., 2014. Radiation impact assessment of naturally occurring radionuclides and magnetic mineral studies of Bharathapuzha river sediments, South India. *Environ. Earth. Sci*., **71**, 3593–3604.

Lecomte K.L., 2006. *Control geomorfológico en la geoquímica de los ríos de Montaña, Sierras Pampeanas, Provincia de Córdoba, Argentina*. PhD Thesis, Facultad de Ciencias Exactas, Físicas y Naturales, Universidad Nacional de Córdoba, Córdoba, Argentina, 279 pp. (in Spanish).

Ligero R.A., Ramos-Lerate I., Barrera M. and Casas-Ruiz M., 2001. Relationships between sea-bed radionuclide activities and some sedimentological variables. *J. Environ. Radioact.*, **57**, 7–19.

Magesh N.S., Jitheshlal K.V., Chandrasekar N. and Jini K.V., 2013. Geographical information system-based morphometric analysis of Bharathapuzha river basin, Kerala, India. *Appl. Water. Sci*., **3**, 467–477.

Magiera T., Strzyszcz Z. and Kostecki M., 2002. Seasonal changes of magnetic susceptibility in sediments from Lake Zywiec (South Poland). *Water Air Soil Pollut.*, **141**, 55–71.

Maher B.A., Thompson R. and Hounslow M.W., 1999. Introduction. In: Maher B.A. and Thompson R. (Eds), *Quaternary Climate, Environments and Magnetism*. Cambridge University Press, Cambridge, U.K., 1–48.

McCubbin D., Leonard K.S., Young A.K., Maher B.A. and Bennett S., 2004. Application of magnetic extraction technique to assess radionuclide-mineral association in Cumbrian shoreline sediments. *J. Environ. Radioact.*, **77**, 11–131.

McLennan S.M., 2001. Relationships between the trace element composition of sedimentary rocks and upper continental crust. *Geochem. Geophys. Geosyst*., **2**, 2000GC000109.

Milliman J.D. and Farnsworth K.L., 2011. *River Discharge to the Coastal Ocean. A Global Synthesis*. Cambridge University Press, Cambridge, U.K.

Montes M.L., Mercader R.C., Taylor M.A., Runco J. and Desimoni J., 2012. Assessment of natural radioactivity levels and their relationship with soil characteristics in undisturbed soils of the northeast of Buenos Aires province, Argentina. *J. Environ. Radioact.*, **105**, 30–39.

Mustonen R., 1985. Radioactivity of fertilizers in Finland. *Sci. Tot. Environ*., **45**, 127–134.

Nikhil Raj P.P. and Azeez P.A., 2012. Morphometric analysis of a tropical medium river system: A case from Bharathapuzha River, Southern India. *Open J. Modern Hydrol.*, **2**, 91–98.

Parizanganeh A.H., Bijnavand V., Zamani A.A. and Hajabolfath A., 2012. Concentration, distribution and comparison of total and bioavailable heavy metals in top soils of Bonab District in Zanjan Province. *Open J. Soil Sci.*, **2**, 123–132.

Peters C. and Dekkers M.J., 2003. Selected room temperature magnetic parameters as a function of mineralogy, concentration and grain size. *Phys. Chem. Earth*, **28**, 659–667.

Petrovský E. and Elwood B.B., 1999. Magnetic monitoring of air, land and water pollution. In: Maher B.A. and Thompson R. (Eds), *Quaternary Climate, Environments and Magnetism*. Cambridge University Press, Cambridge, U.K., 279–322.

Raj N. and Azeez P.A., 2009. Spatial and temporal variation in Surface water chemistry of a tropical river, the river Bharathapuzha, India. *Current Sci.*, **96**, 245–251.

Ramasamy V., Paramasivam K., Suresh G. and Jose M.T., 2014. Role of sediments characteristcs on natural radiation level of the Vaigai river sediment, Tamilnadu, India. *J. Environ. Radioact.*, **127**, 64–74.

Rapela C.W., 1982. Aspectos geoquímicos y petrológicos del Batolito de Achala, provincia de Córdoba. *Revista de la Asociación Geológica Argentina*, **37**, 314–330 (in Spanish).

Righi S., Lucialli P. and Bruzzi L., 2005. Health and environmental impacts of a fertilizer plant - Part I: assessment of radioactive pollution. *J. Environ. Radioact*., **82**, 167–182.

Roselli C., Desideri D., Assunta Meli M. and Feduzi L., 2010. Sequential extraction for the leachability evaluation of phosphate fertilizers. *Microchem. J.*, **95**, 373–376.

Sakthimurugan S., 2007. *Groundwater Information Booklet of Thrissur District, Kerala State*. Central Ground Water Board, Thiruvananthapuram, Kerala, India (http://cgwb.gov.in /District_Profile/Kerala/Thrissur.pdf).

Sandeep K., Shankar R. and Krishnaswamy J., 2011. Assessment of suspended particulate pollution in the Bhadra River catchment, Southern India: an environmental magnetic approach. *Environ. Earth Sci.*, **62**, 625–637.

Savci S., 2012. An agricultural pollutant: chemical fertilizer. *Int. J. Environ. Sci. Develop.*, **3**, 77–80.

Scholger R., 1998. Heavy metal pollution monitoring by magnetic susceptibility measurements applied to sediments of the river Mur (Styria, Austria). *Eur. J. Environ. Eng. Geophys*., **3**, 25–37.

Scholten L.C. and Timmermans C.W.M., 1996. Natural radioactivity in phosphate fertilizers. *Fertil. Res.*, **43**, 103–107.

Sreela S.R., 2009. *An Integrated Study on the Hydrogeology of Bharathapuzha River Basin, South West Coast of India*. Ph.D Thesis, Cochin University of Science and Technolology, Cochin, Kerala, India.

Sreela R., Rej S., Girish G., Rajesh R. and Kurian S., 2012. A numerical weighted parameter rating (WPR) for artificial groundwater recharging in Bharathapuzha river basin: Southern India. *Int. J. Earth Sci. Eng.*, **5**, 268–275.

Suresh G., Ramasamy V., Meenakshisundaram V., Venkatachalapathy R. and Ponnusamy V., 2011. A relationship between the natural radioactivity and mineralogical composition of the Ponnaiyar river sediments, India. *J. Environ. Radioact.*, **102**, 370–377.

Thompson R. and Oldfield F., 1986. *Environmental Magnetism*. Allen & Unwin Publishers Ltd., London, U.K., 225 pp.

Tume P., Bech J., Longan L., Tume L., Reverter F. and Sepúlveda B., 2006. Trace elements in natural surface soils in Sant Climent (Catalonia, Spain). *Ecol. Eng.*, **27**, 145–152.

UNSCEAR, 2000. *United Nations Scientific Committee on the Effect of Atomic Radiation. Sources and Effects of Ionizing Radiation*. Report to General Assembly. United Nations Organization, New York.

Veiga R., Sancher N., Anjos R.M., Macario K., Bastos J., Iguatemya M., Aguiar J.G., Santos A.M.A., Mosquera B., Carvalho C., Baptista F.M. and Umisedo N.K., 2006. Measurement of natural radioactivity in Brazilian beach sands. *Radiat. Meas*., **4**, 189–196.

Yafa C. and Farmer J.G., 2006. A comparative study of acid-extractable and total digestion methods for the determination of inorganic elements in peat material by inductively coupled plasma-optical emission spectrometry. *Analytica Chimica Acta*, **557**, 296–303.

Yang T., Liu Q., Chan L. and Liu Z., 2007. Magnetic signature of heavy metals pollution of sediments: Case study from the East Lake in Wuhan, China. *Environ. Geol.*, **52**, 1639–1650.

Zhang C.X., Qiao Q., Piper J.D.A. and Huang B., 2011. Assessment of heavy metal pollution from a Fe-smelting plant in urban river sediments using environmental magnetic and geochemical methods. *Environ. Pollut.*, **159**, 3057–3070.